TECHNICAL REPORT NO. 12

TO

The Office of Naval Research
Contract No. N000014-86-K-0381

ADVANCED PROCESSING AND PROPERTIES OF HIGH PERFORMANCE ALLOYS

D. A. Koss

Department of Materials Science and Engineering
The Pennsylvania State University
University Park, PA 16802

Report for the period 1 January 1988 - 31 December 1988

SECURITY CLASSIFICATION OF THIS PAGE *(When Data Entered)*

REPORT DOCUMENTATION PAGE		READ INSTRUCTIONS BEFORE COMPLETING FORM
1. REPORT NUMBER Technical Report No. 12	2. GOVT ACCESSION NO.	3. RECIPIENT'S CATALOG NUMBER
4. TITLE *(and Subtitle)* Advanced Processing and Properties of High Performance Alloys		5. TYPE OF REPORT & PERIOD COVERED 6. PERFORMING ORG. REPORT NUMBER
7. AUTHOR(s) D. A. Koss		8. CONTRACT OR GRANT NUMBER(s) N00014-86-K-0381
9. PERFORMING ORGANIZATION NAME AND ADDRESS Department of Materials Science and Engineering The Pennsylvania State University University Park, PA 16802		10. PROGRAM ELEMENT, PROJECT, TASK AREA & WORK UNIT NUMBERS
11. CONTROLLING OFFICE NAME AND ADDRESS Office of Naval Research 800 N. Quincy St. Arlington, VA 22217		12. REPORT DATE April 1989 13. NUMBER OF PAGES 31
14. MONITORING AGENCY NAME & ADDRESS*(if different from Controlling Office)*		15. SECURITY CLASS. *(of this report)* 15a. DECLASSIFICATION/DOWNGRADING SCHEDULE

16. DISTRIBUTION STATEMENT *(of this Report)*

Distribution of this document is unlimited.

17. DISTRIBUTION STATEMENT *(of the abstract entered in Block 20, if different from Report)*

18. SUPPLEMENTARY NOTES

19. KEY WORDS *(Continue on reverse side if necessary and identify by block number)*

Processing, Fracture mechanisms, Void/Pore linking, low cycle fatigue, Cu-Nb alloys

20. ABSTRACT *(Continue on reverse side if necessary and identify by block number)*

Progress is reviewed for a research program whose purpose is to establish a broad-based understanding of the application and consequences of advanced processing techniques, especially as they influence the strength and fracture resistance of high performance structural alloys. While some of the research is specific to certain alloy systems, much of the program constitutes fundamental study of the deformation and fracture of engineering alloys containing processing-induced defects. Progress for the period January 1, 1988, to December 31, 1988, is reviewed for the following projects within the program:

DD FORM 1 JAN 73 1473 EDITION OF 1 NOV 65 IS OBSOLETE

SECURITY CLASSIFICATION OF THIS PAGE *(When Data Entered)*

A

20. Continued

(1) the influence of porosity on low cycle fatigue,

(2) the mechanism of strain-induced void/pore linking during ductile fracture, and

(3) the processing and properties of Cu-Nb microcomposites.

Copper; mechanical metallurgy; physical properties, low cycle fatigue, metal fatigue; Niobium; Copper; Alloys; (A-1, a

Accession For	
NTIS GRA&I	☑
DTIC TAB	☐
Unannounced	☐
Justification	
By	
Distribution/	
Availability Codes	
Dist	Avail and/or Special
A-1	

ADVANCED PROCESSING AND PROPERTIES OF HIGH PERFORMANCE ALLOYS

INTRODUCTION

Advanced structural systems require a new generation of high performance materials which exhibit dramatic improvements in both strength and fracture resistance over a wide range of temperatures and environments. These materials are increasingly dependent on advanced processing techniques. For example, as will be described in our Cu-Nb project, the application of rapid solidification processing must be used to obtain ultra-fine, stable microstructures in powder form; these in turn require additional processing (usually by powder metallurgy techniques) to achieve fully dense components with superior properties. Other examples can also be readily cited.[1-3]

A fundamental problem in advanced alloy technology is that the rate of application of new processing methods exceeds the basic knowledge base necessary to anticipate fully the resulting behavior of the component in service. Thus, while novel alloy microstructures are created through advanced processing techniques, the promise of improved properties is usually accompanied by the potential for a new set of problems. For instance, rapidly solidified dispersion hardened alloys may exhibit superior short time tensile strengths but inadequate high temperature creep strength due to the stabilization of fine grain sizes and the resulting enhanced grain boundary sliding. As a result, despite notable improvements in some aspects of the material's properties, long term/high temperature in-service reliability may be impaired.

The primary purpose of the present research is to provide a broad-based understanding of the applications and consequences of certain advanced processing techniques when used to create new high performance alloys. The research has ranged in scope from fundamental studies of the mechanisms of void or pore linking during ductile fracture and the influence of porosity on low cycle fatigue to the processing-property relationships in Cu-Nb alloys. The present report summarizes progress in the areas of

research for the period 1/1/88 to 12/31/88 performed under the auspices of Contract No. NOOO14-86-K-0381. The research areas are as follows:

(1) the influence of porosity on low cycle fatigue,

(2) the mechanism of strain-induced void/pore linking during ductile fracture, and

(3) processing and properties of Cu-Nb alloys.

A significant impact of the above research is the educational experience derived by the graduate students involved. The following students have been a part of this ONR program during the period cited: Dale Gerard, Ph.D., November, 1988; Kevin Zeik, Ph.D. candidate; and Andrew Geltmacher, M.S. candidate.

SUMMARY OF RESEARCH

1. The Influence of Porosity on the Low Cycle Fatigue of Metals
(with Dale Gerard, Ph.D., November, 1988)

The in-service performance of powder-processed as well as cast materials is frequently limited by the presence of processing defects, notably porosity. Numerous investigations have examined the deleterious effects of porosity on high cycle fatigue and uniaxial tension behavior; see for example refs. 4-8. The reductions in high cycle fatigue life of porous specimens have been attributed to local stress concentrations near pores which result in localized slip even though the nominal stress remains elastic. Although there have been many studies investigating the effects of porosity on high cycle fatigue behavior of metals, there have been no fundamental studies examining the effects of porosity on low cycle fatigue behavior. This is significant since the resistance of metals to low cycle fatigue failure, wherein the material is fully plastic, is often quite different than the response to high cycle fatigue when the nominal applied stress is elastic.

The purpose of this investigation is to examine in a detailed manner the influence of rounded porosity on low cycle fatigue behavior. The study has been performed such that the macroscopic effects are identified and interpreted in terms of the micromechanisms of failure. Powder-processed titanium containing up to 6% rounded porosity (both isolated and continuous pores) has been used as a model system. Although this study is based on powder-processed materials,

the results should also apply to cast materials which frequently contain residual porosity, or to those alloy/composite systems which readily form voids at small strains due to poor interfacial bonding or fiber fracture.

The influence of porosity on low cycle fatigue LCF has been studied using powder-processed titanium specimens tested at total strain amplitudes of 0.75 and 1.5% at 25°C. From a macroscopic standpoint, the following trends are most significant:

a. Porosity significantly influences the cyclic stress-strain behavior. For example, when compared to the cyclic flow response of fully dense titanium, even low levels of porosity (0.4%) cause the material to behave cyclically as if it were being subjected to significantly higher strain amplitudes. This is interpreted to result from an enhanced level of localized plasticity which develops near the pores.

b. As shown in Fig. 1, low cycle fatigue life deteriorates with increasing volume fraction of porosity, strain amplitude, and especially when the porosity becomes interconnected. Even small amounts of porosity have a significant effect on LCF. For example, the presence of just 0.4% porosity decrease the LCF life by more than a factor of three at 1.5% total strain amplitude.

In order to evaluate mechanism of low cycle fatigue in the presence of pores, the influence of porosity on the individual stages of the fatigue failure process has been thoroughly examined. In this investigation, fatigue failure is described by a four stage process consisting of the number of cycles for (1) a 15 μm microcrack to initiate, (2) microcrack(s) (i.e. short cracks) to grow and (3) link into a macrocrack, and (4) the macrocrack to propagate to failure. If any of the failure stages are accelerated by the presence of pores, a reduction in the low cycle fatigue life is eminent.

Fig 2a illustrates that the pore-induced acceleration is especially large for microcrack initiation. The acceleration of microcrack initiation appears to be essentially independent of the porosity levels and strain amplitudes examined, but it is sensitive to the interconnectivity of the porosity. Specifically, 6% interconnected porosity accelerates crack initiation by a factor of about 100, compared to a factor of 10 for isolated porosity. Thus, while microcracks initiate in 800

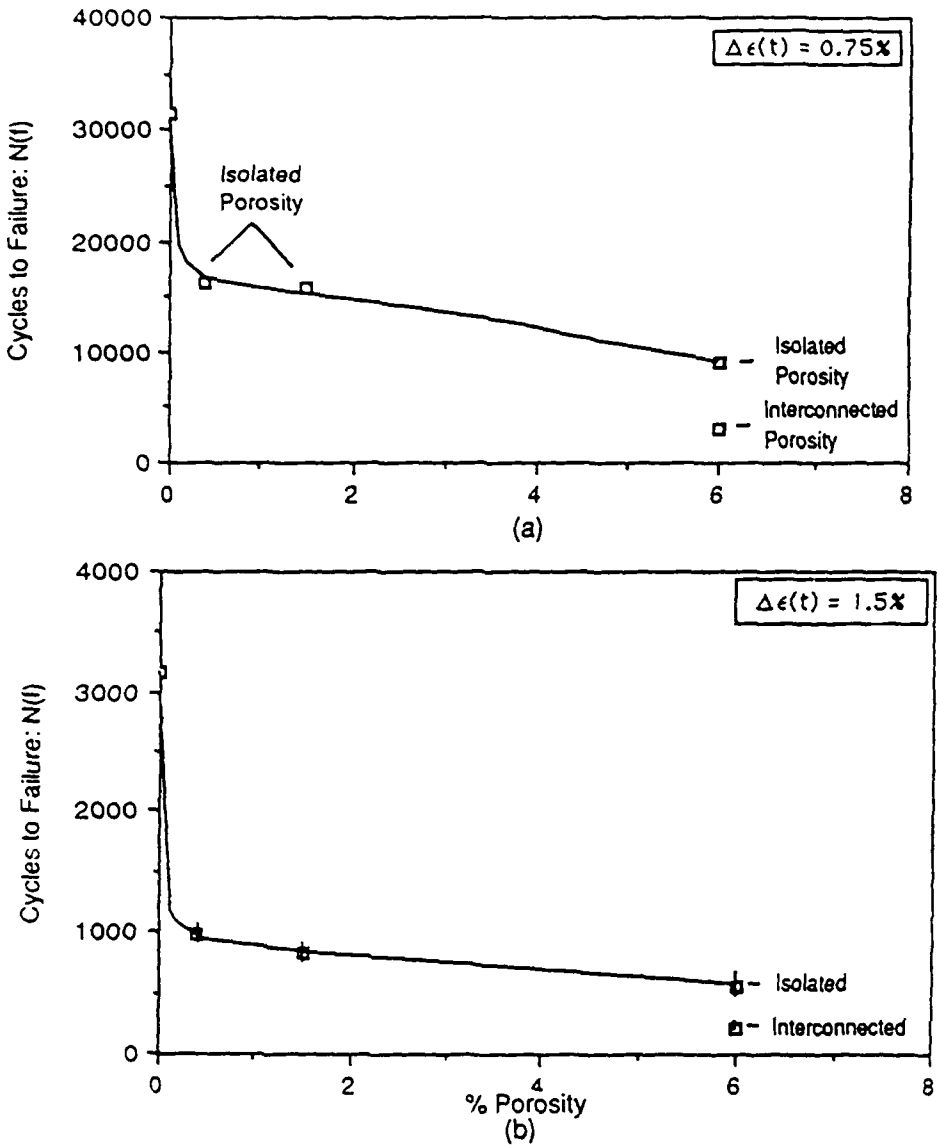

Figure 1. The influence of porosity on low cycle fatigue life for titanium subjected to total strain amplitude testing at (a) 0.75%, and (b) 1.5%.

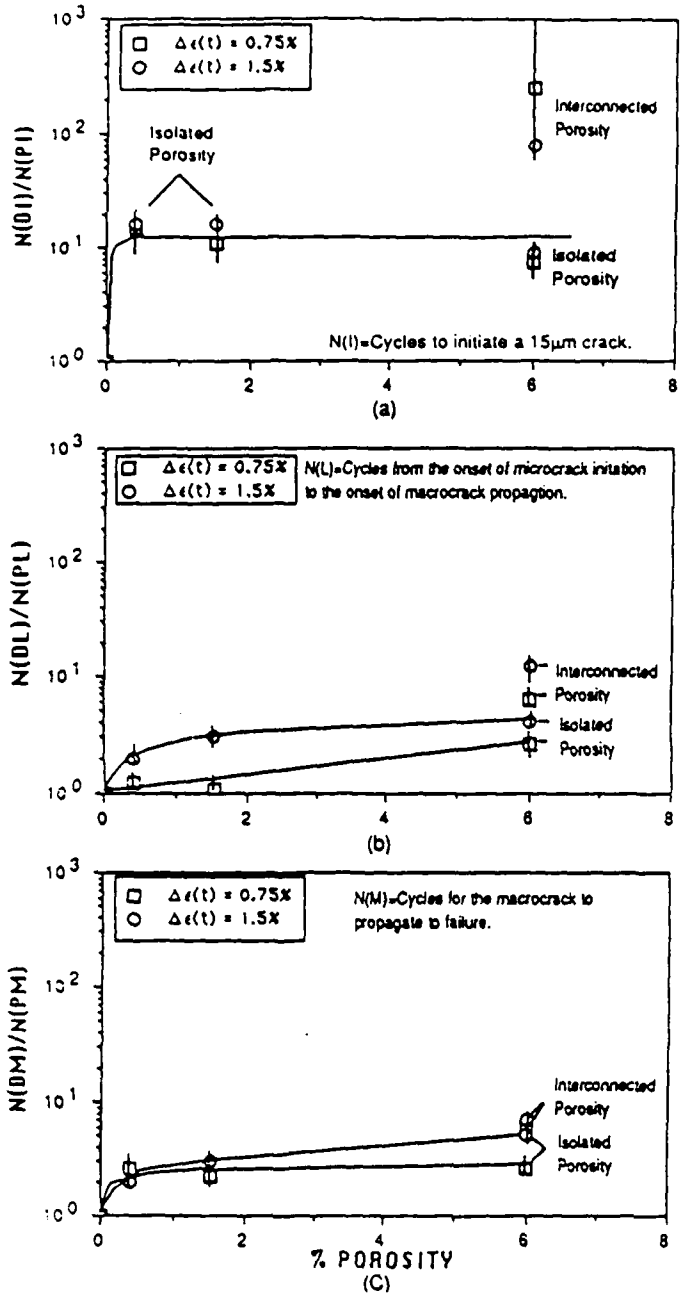

Figure 2. The number of cycles for the fully dense titanium in a particular failure stage normalized to those for porous materials for (a) microcrack initiation, (b) microcrack growth and linking, and (c) macrocrack propagation. The ratios indicate the effect that porosity has on accelerating each of the stages of fatigue failure when compared to the fully dense titanium.

cycles in the fully dense titanium at 1.5% total strain amplitude, only 9 cycles are required to initiate a similar crack at 6% interconnected porosity!

Both the microcrack growth/linking and the macrocrack growth stages, which are illustrated in Fig. 2b and c respectively, also accelerate with increasing porosity level, strain amplitude and degree of interconnectivity of the porosity. In the case of microcrack growth and linking (Fig. 2b), the acceleration is most pronounced at large porosity levels, and especially for the case of interconnected porosity. Macrocrack growth (Fig. 2c) appears roughly a factor of 2-3 times faster when the isolated pores are present; again the interconnected porosity accelerated this stage more than the isolated porosity. The individual stages of the LCF failure process will now be examined in detail.

With regard to microcrack initiation, the following experimental observations/conclusions are pertinent:

(a) The enhancement of microcrack initiation due to porosity results in significant reductions in low cycle fatigue life. Fig. 2 indicates that, for all the levels of porosity examined, the number of cycles necessary to initiate a 15 micron crack decreased by roughly an order of magnitude or more.

(b) Microcracks always initiate at pores. Thus, the acceleration of microcrack initiation is a result of pore-induced plastic zones which create locally high regions of plastic strain extending roughly two to three pore radii beyond the edge of a pore on the plane of maximum strain concentration.

(c) For the isolated-porous materials, the enhancement of microcrack initiation is essentially independent of the porosity levels at the strain amplitude examined, see Fig. 2.

(d) When the porosity is interconnected, the microcrack initiation process is further enhanced as a result of the pores having a higher aspect ratio than the isolated porous materials.

An analysis of pore-induced microcrack initiation is successfully performed on the following basis:

(a) The formation of the plastic zones near pores on the free surface of a plastically deforming matrix have been experimentally and theoretically modeled utilizing a through-thickness hole in metals deforming under plane stress conditions. Excellent agreement is obtained between experimentally measured and theoretically estimated strain profiles adjacent to the holes based on a modified Neuber analysis.[9] Furthermore, agreement continues to be good even when the matrices are subjected to low cycle fatigue deformation. A significant observation is that the strain profiles obtained adjacent to a hole indicate that no local strain accumulation occurs during LCF until approximately 80% of the fatigue life local to the hole.

(b) Using a Manson-Coffin relationship[10,11] as a local failure criterion in conjunction with a cumulative damage law, the number of cycles to initiate a 15 μm crack can be predicted from estimates of the maximum strain amplitudes near pores, as determined by the modified Neuber analysis.[9] Fig. 3 also indicates that the predictions of this analysis are in excellent agreement with the experimental data over a range of pore contents and at both strain amplitudes. It should be noted that this is a general analysis and applies to LCF crack initiation in any metal containing porosity of arbitrary shapes which can be described by stress concentration factors; only the cyclic stress-strain response of the matrix needs to be known.

With regard to the growth of short cracks, in the presence of porosity, the following characteristics are most significant:[12]

(a) Isolated rounded porosity temporarily accelerates short fatigue crack growth rates as a result of large plastic strains within the plastic zones of the pores. Outside of the plastic zones, which scale with the pore size, short cracks propagate at rates which are similar to those which are expected in a fully dense material. Over the range of porosity examined, most of the short crack propagation occurs outside of the pore-induced plastic zones and thus the overall growth rates are not significantly influenced in the presence of porosity; see Fig. 4. However, for the case of 6% interconnected porous specimens tested at 1.5% total strain amplitude, the short fatigue cracks propagate at rates two to ten times faster than in the fully dense and isolated-porosity specimens.

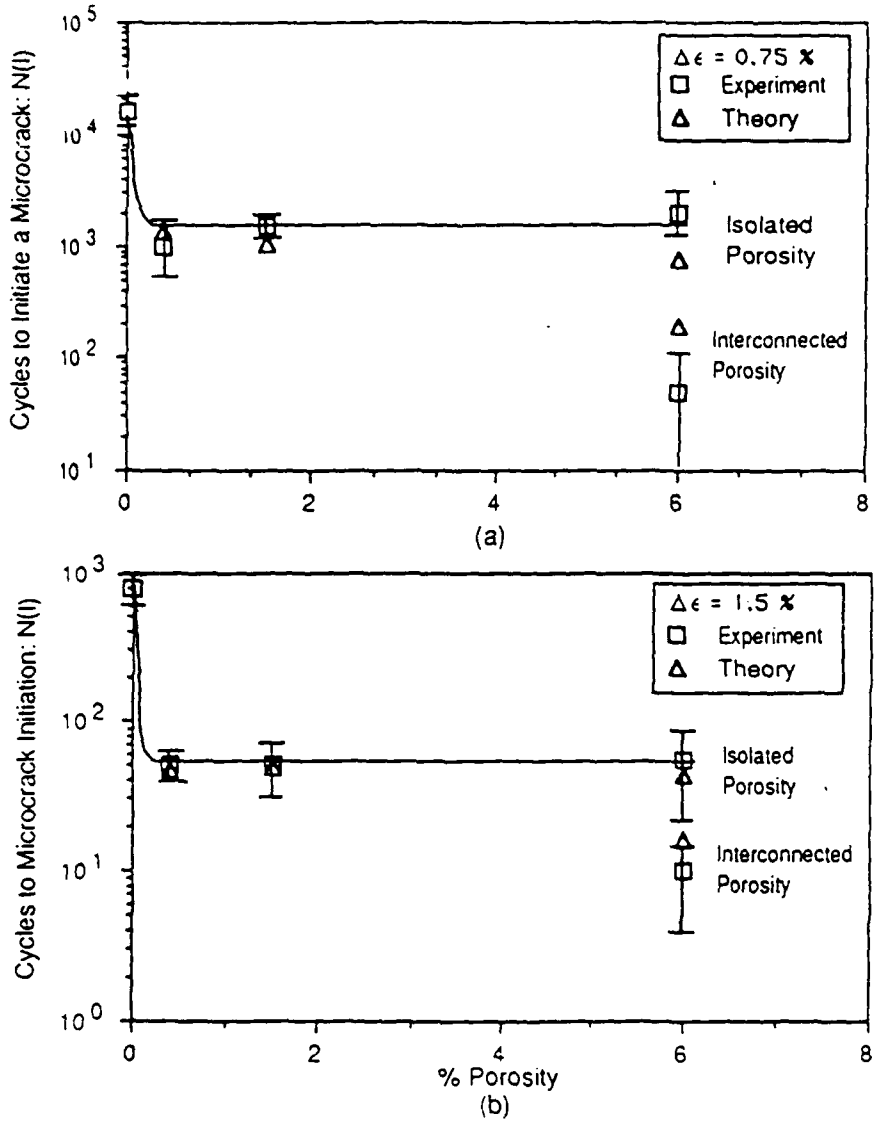

Figure 3. A comparison of the experimental results and theoretical predictions for the number of cycles to initiate a 15μm crack in the fully dense and porous materials during total strain amplitude at (a) 0.75% and (b) 1.5%.

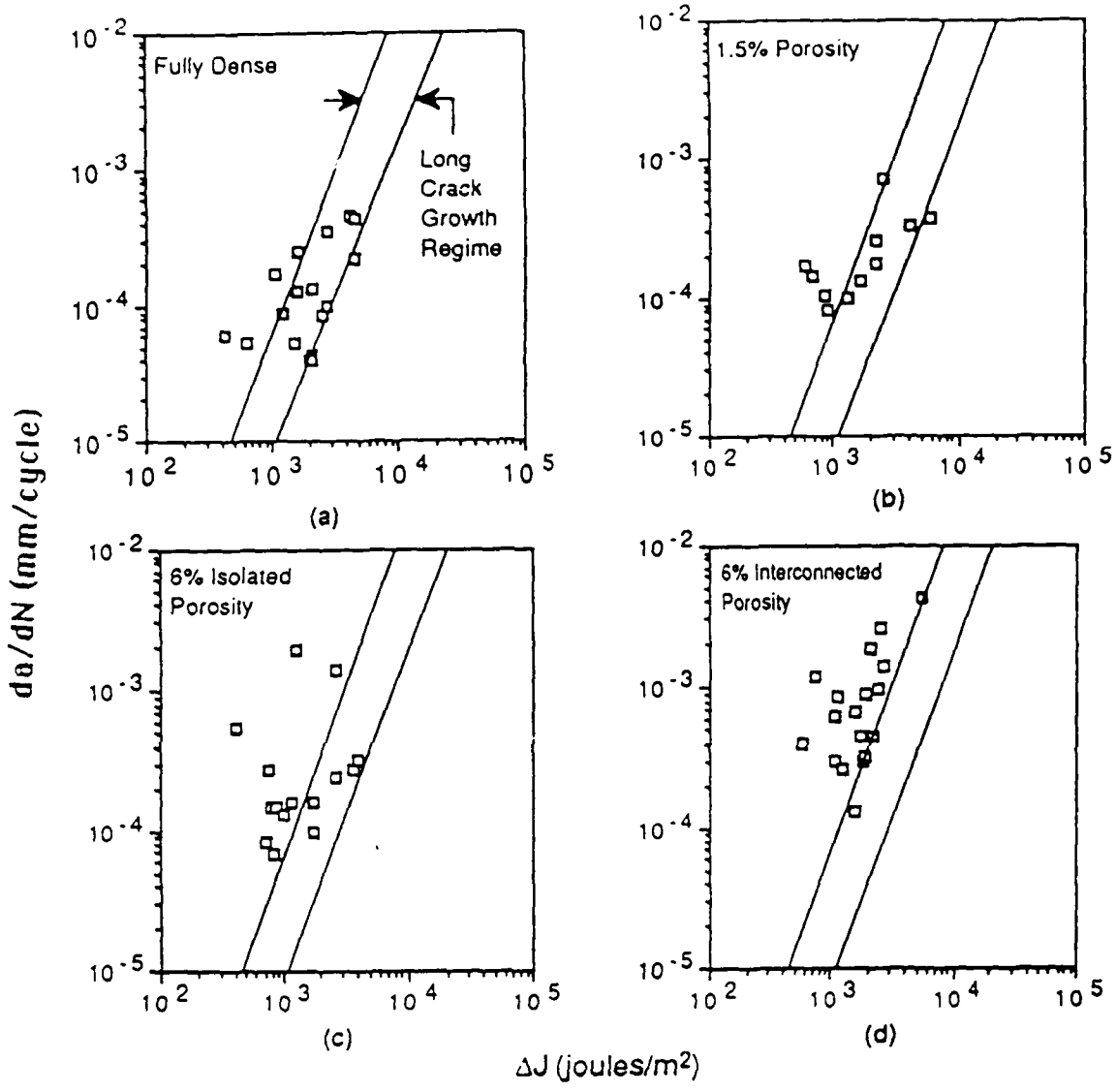

Figure 4. The dependence of short crack growth rates on ΔJ as measured during 1.5% total strain amplitude testing for titanium which has (a) 0% porosity, (b) 1.5% isolated porosity, (c) 6% isolated porosity, and 9d) 6% interconnected porosity. The two solid lines in each plot indicate an extrapolated range of the long crack growth data obtained by Robinson and Beevers for fully dense titanium of similar purity to that used in this investigation.

This effect appears to be a result of the continuous plastic zones which are present in the material containing the interconnected porosity.

(b) Crack closure of short cracks has been observed to occur at the crack-tip only at highly compressive loads. Portions of the crack behind the tip appeared to remain open during the entire cycle. The short crack-tips open early in the tensile loading portion (between 0 and 60 MPa) of the cycle, "peeling" open from the center toward the tip of the crack. It appears that porosity does not influence short crack closure during high-strain fatigue testing.

The role of porosity in microcrack linking during the LCF of porous materials may be understood as follows:

(a) The microcrack linking process is accelerated by porosity as a result of a higher density of microcracks. Thus, the principal effect of porosity on microcrack linking is to increase in density of the microcracks due to the additional crack initiation sights (i.e. pores) in the porous materials.

(b) When comparing the acceleration of the microcrack linking process directly among the different porosity levels, only minimal increases in the linking rate which observed when the isolated-porosity level is increased from 0.4% to 6%. This is attributed to a saturation density of microcracks which is very similar over this porosity range.

(c) The influence of porosity on microcrack linking is significantly less at the 0.75% total strain amplitude. This appears to be a result of a much lower density of microcracks being initiated throughout the fatigue life for all the conditions which have been examined.

(d) Because of the interaction between short crack growth and microcrack linking, a rigorous theoretical analysis of the number of cycles to grow and link microcracks into a macrocrack could not be performed. However, the following semi-quantitative analysis provides insight into the microcrack growth linking processes. At total strain amplitude testing of 1.5%, the mean crack length of all the cracks present on the specimen surface is observed to have a value (140 ± 20 μm) at the commencement of long crack growth; see Fig. 5. Since a macrocrack is roughly 1.4 mm when it begins to be the sole crack which dominates crack growth, the mean

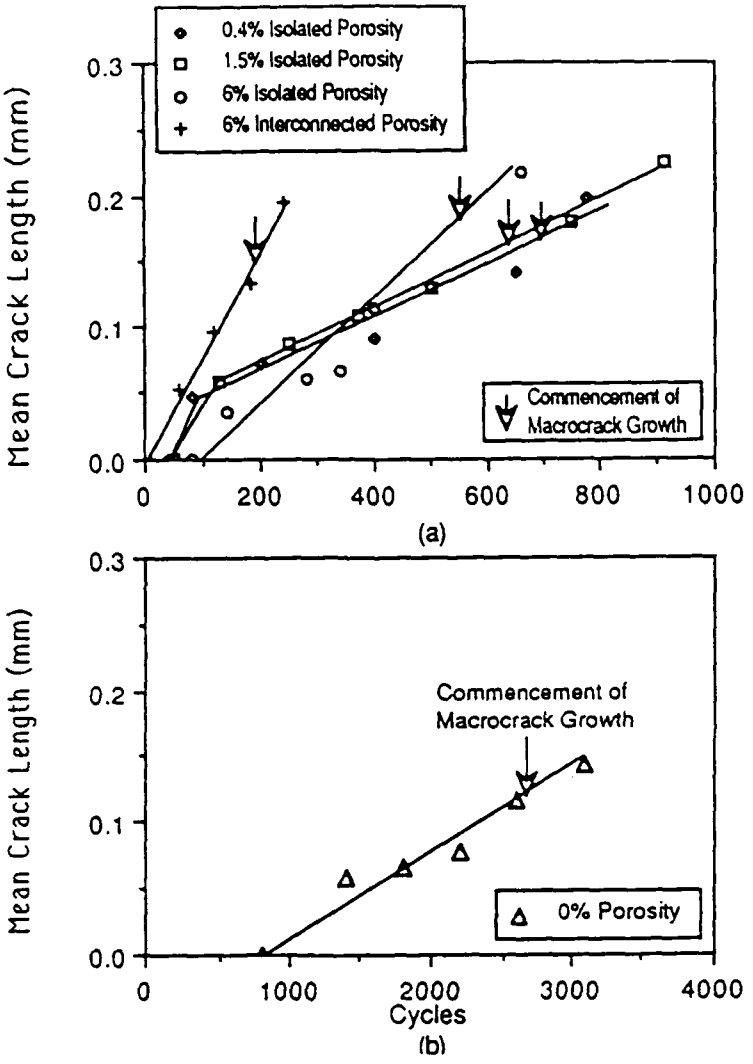

Figure 5. The mean crack length for the microcracks examined at various stages of fatigue life for (a) the porous materials, and (b) the fully dense titanium. The arrows indicate the onset of macrocrack propagation.

crack size is approximately one-tenth the length of the dominant macrocrack. Furthermore, the mean crack length, which reflects concurrent short crack growth and liking, is experimentally observed to depend linearly on the total number of cycles. Based on this information, we are able to estimate the number of cycles from crack initiation to the onset of macrocrack propagation for both the porous and fully dense materials. The agreement between predicted and observed cyclic life is good.

Macrocrack propagation is affected by porosity in the following manner:

(a) Porosity accelerates the overall macrocrack growth rates, as approximated by the number of cycles for a macrocrack to propagate through the specimen, by factors of roughly two to four. The effect of porosity on the enhancement of macrocrack propagation rates become slightly more pronounced with increasing strain amplitude and when porosity is interconnected.

(b) The closure stress for macrocracks is not significantly influenced by the presence porosity during high-strain fatigue.

(c) By incorporating a *lineal roughness parameter, porosity-induced increases in the* macrocrack growth rates are quite large for the 6% porous materials when the actual distances over which the crack propagates are considered. At the lower porosity levels the macrocrack growth rates are only nominally larger when the lineal roughness parameter is taken into consideration.

(d) As shown schematically in Figure 6, a qualitative model has been developed which physically accounts for the accelerated growth rates of macrocracks in the porous materials. The model assumes minimal differences in crack closure behavior between the porous and fully dense materials, as is observed experimentally. The model is based on the concept that the acceleration of macrocrack growth in the presence of porosity at large strain amplitudes is a result of the interaction of the crack-tip plastic zone with the pore-induced plastic zones resulting in shear instabilities. These shear instabilities contribute to an additional crack growth component. Thus with the minimal differences in crack closure observed between the porous and fully dense materials, an acceleration in long crack growth rates subsequently occur.

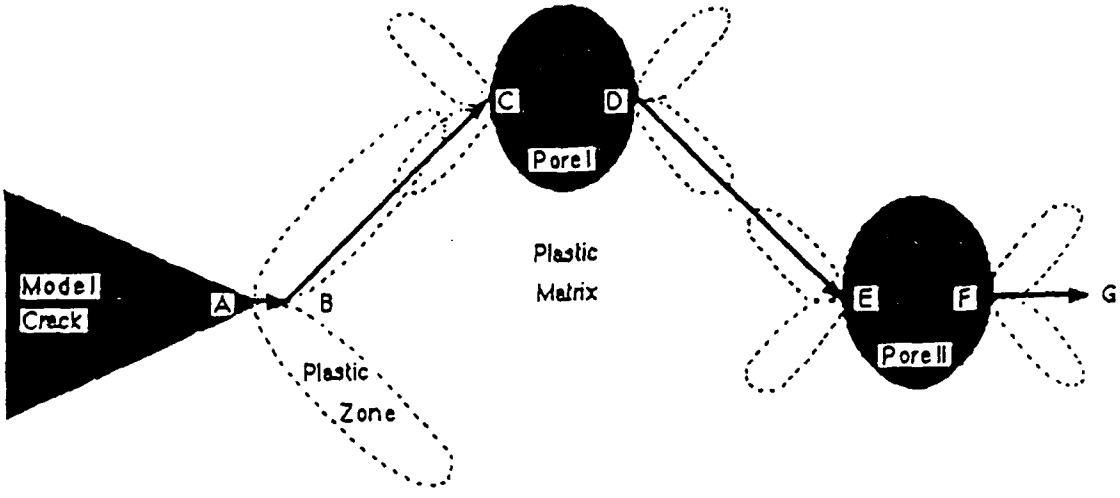

Figure 6. Illustration of a mode 1 low cycle fatigue crack propagating through a plastic matrix containing porosity. The crack is predicted to propagate along the path designated by the line segments described by the points 'A' thru 'G'.

2. The Mechanism of Strained-Induced Void/Pore Linking During Ductile Fracture [with Andrew Geltmacher, M.S. candidate]

The presence of pre-existing porosity and the subsequent process of pore linking during deformation is known to have a strong effect on the ductile fracture of porous materials (see for example, ref. 8). Similarly, strain-induced void linking is an integral part of the ductile fracture process. Although differing in their origin, pores and voids link in a similar manner during low temperature deformation, and thus failure of a porous or "voided" material may be examined together in a single analysis. Even though void/pore linking is a very important step in the process of ductile fracture, it has not been properly understood until our recent studies.[13-15] The reason for this situation is that nearly all of the previous work on void/pore growth and linking assumed regular arrays of holes or cavities[16-22] and an arbitrary, geometrically based void linking criteria.[23-25] The present study is based on modeling three-dimensional arrays of pores or voids by a two-dimensional random distribution of circular through-thickness holes. The distribution of holes or "hole microstructure" may be characterized by three parameters: (a) the area fraction, (b) the hole size, and (c) the minimum interhole spacing, which controls the degree of hole clustering. A focus of the study is to examine the void/pore linking process by determining the failure sequence of tensile specimens containing arrays of holes. An important feature of this program is the strong interaction between experimental studies and computer simulation. As will be demonstrated, both of these aspects are necessary in order to define the mechanism of void/pore linking during ductile fracture.

The experimental studies indicate a strong correlation between minimum interhole spacing and the mechanical properties of tensile specimens containing hole microstructures. Both the strength and ductility of the specimens were found to increase as the minimum interhole spacing was increased or the degree of clustering decreased.[13-15] These studies also indicate that specimens exhibit a dramatic decrease in ductility on changing from

regular to random arrays of holes. Figure 7 illustrates the strong effects of the minimum interhole spacing and regular versus random arrays of holes on the fracture of low carbon steel sheet. Experimental studies also indicate that the strain hardening of a material is very important in the void/pore linking process. This makes any prediction of void linking based on an arbitrary, geometric linking criteria[23-25] quite inadequate. For example, a void/hole linking criterion which provides a reasonable fracture strain for one material with a given void/pore distribution will very likely be incorrect for another material with differing strain hardening behavior or void/pore distribution.

The observed effects of the experimental studies can be readily understood through the use of a proposed physical model.[13,14] In the model, the fracture mechanism is a consequence of a four-step process:

First, local strain gradients develop near individual pores at small microscopic strains;

Second, upon further straining, failure of the ligament between closely spaced pores occurs due to flow localization. An elongated cavity is created by the ligament failure. Due to its eccentric shape, this cavity further localizes flow along its major axis;

Third, successive linking to additional pores occurs in a manner which is controlled by the spatial distribution of pores adjacent to those which have linked. Pore clustering is especially important in this stage as repeated linking results in increased strain concentration;

Fourth, the final stage of pore linking is triggered when a sufficient number of pores have linked to create an imperfection-initiated macroscopic flow instability or crack-like defect. Again pore clustering is important as the generation of large local strains occur and percolation of the linking by a "void sheet" mechanism can occur.

This step-wise process of void linking lends itself to simulation by a computer model. The computer model also relies on experimental data of the strain localization near (a) isolated single holes, (b) pairs of unlinked holes, (c) pairs of linked holes, and (d) by extension of (c), multiple holes which have linked. The experimental measurements, which have been performed on 1100 aluminum and 70-30 brass sheet, have been fit to empirical equations, which are similar in form to those which describe the elastic stress fields.[26] These equations are then used to describe the strain localization of the above

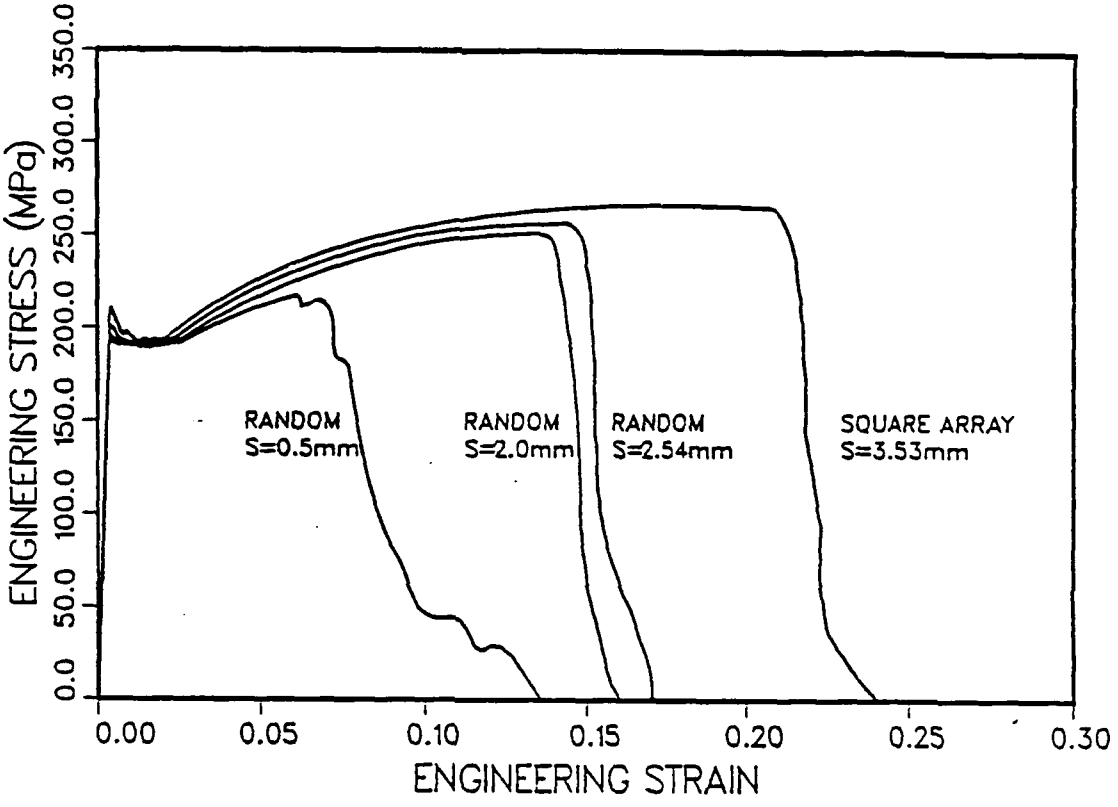

Figure 7. Engineering stress-strain behavior as a function of the minimum interhole spacing, (s), and the type of hole array for low carbon steel sheet. Data of Magnusen et al.[14].

conditions in terms of hole parameters, material properties, and the applied strain. The computer model also relies on a critical strain criterion for the failure of the ligament between adjacent holes. For the sheet material, this criterion is a critical thickness strain, which may be readily understood in terms of sheet failure theory.[27,28] It is important to note that the simulation uses no adjustable parameters other than those which experimentally describe the plasticity near the holes and the failure criterion for hole linking.

Figure 8 is an example of the agreement between the computer simulation and the experimental results for 1100 aluminum. For each point in the simulation, a minimum of ten computer runs were averaged in order to obtain statistically reliable predictions. In view of the absence of adjustable parameters in the computer simulation, the agreement between the predictions of the simulation and the experimental data is reasonable. Similar agreement is obtained for the higher strain-hardening, 70-30 brass, as shown in Figure 9.

In light of the reasonable agreement between prediction and experimental results, the computer simulation has recently been used to investigate the effects of the specimen shape on ductile fracture.[29] Figure 10 illustrates the three specimen shapes used. All three specimen shapes have identical gage section areas of 3225 mm^2 but their length-to-width ratios vary from 1:1 to 20:1. Figures 8 and 9 indicate that specimen shape has several effects on the fracture of porous metals. First, ductility depends on specimen shape but only at small area fractions of porosity. In general, ductility decreases as the specimen's length-to-width ratio is increased. Second, the decrease in ductility with increasing length-to-width ratio of the specimen noted above is more pronounced when the pores are clustered. This latter effect is illustrated by comparing Figures 8a to 8b and 9a to 9b, where Figures 8a and 9a represent the distributions with a higher degree of pore clustering. The computer simulation also predicts that the scatter of the ductility values is significantly greater in specimens with a high length-to-width ratio than for those with a low length-to-width ratio. The degree of scatter within the ductility data is shown in Figure 11 through

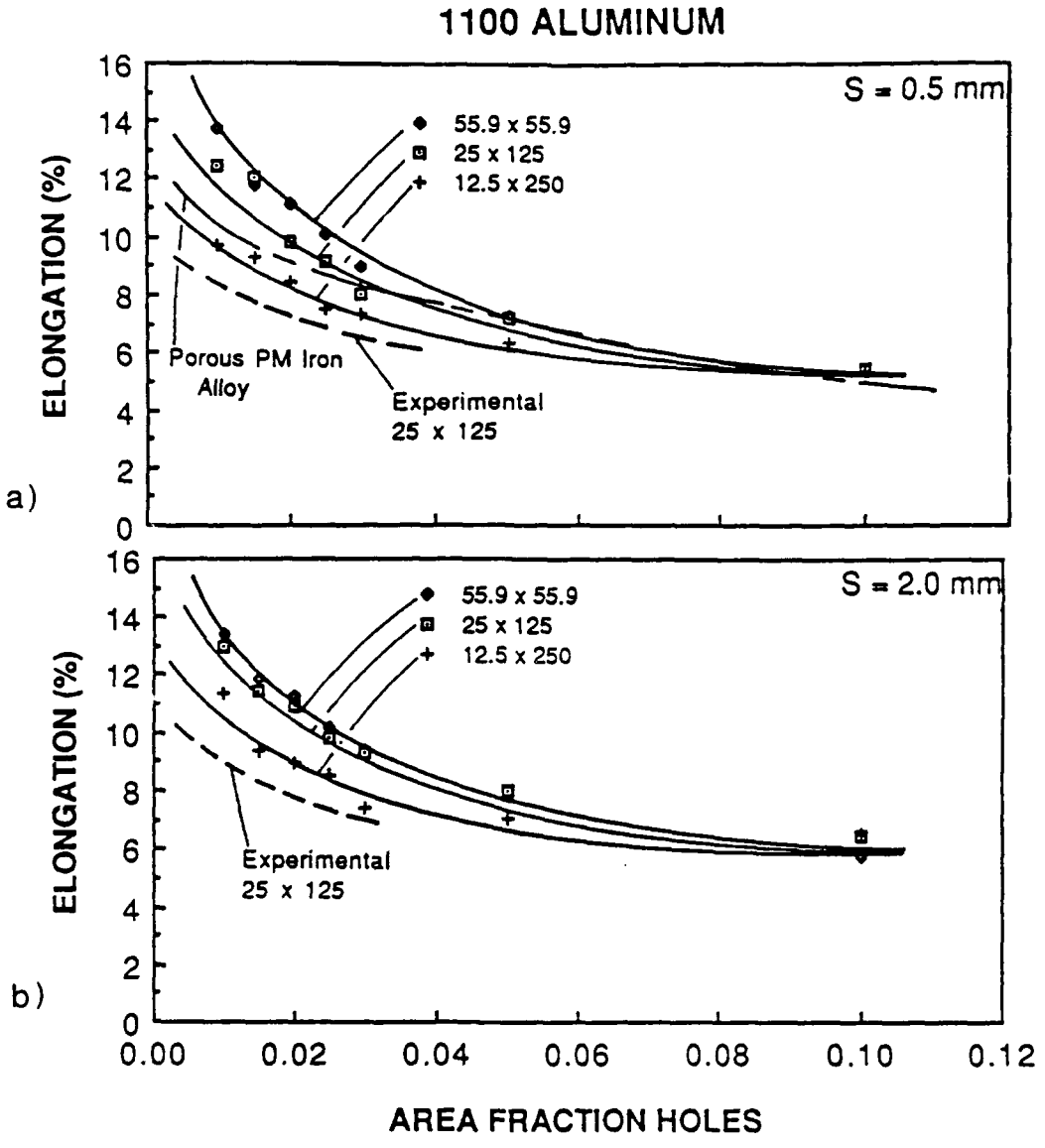

Figure 8. The dependence of the elongation to failure on the area fraction holes for 1100 aluminum. The diameter of the holes is 2.0 mm and the minimum allowable hole spacing are (a) 0.5 mm and (b) 2.0 mm. Data from the computer simulation are shown for specimen sizes of 55.9x55.9, 25x125 and 250 mms. The curves from the experimental model shown are from ref. [13,14] and in (a) the curve for porous PM iron is from ref. [30].

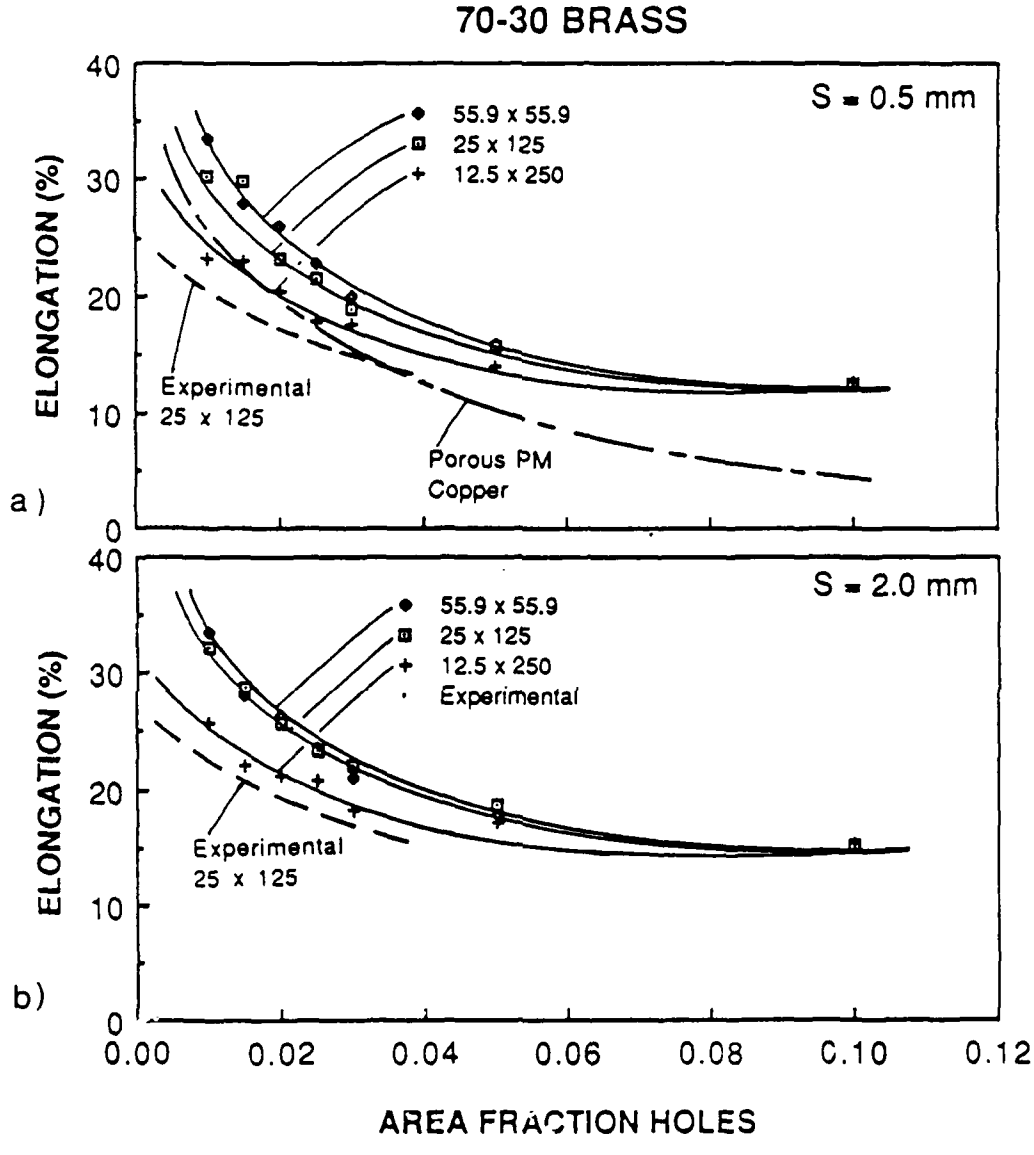

Figure 9. The dependence of the elongation to failure on the area fraction holes for 70-30 brass. The diameter of the holes is 2.0 mm and the minimum allowable hole spacings are (a) 0.5 mm and (b) 2.0 mm. Data from the computer simulation are shown for specimen sizes of 55.9x55.9, 25x125 and 12.5x250 mms. The curves from the experimental model shown are from ref. [13,14] and in (a) the curve for porous PM copper is from ref. [31].

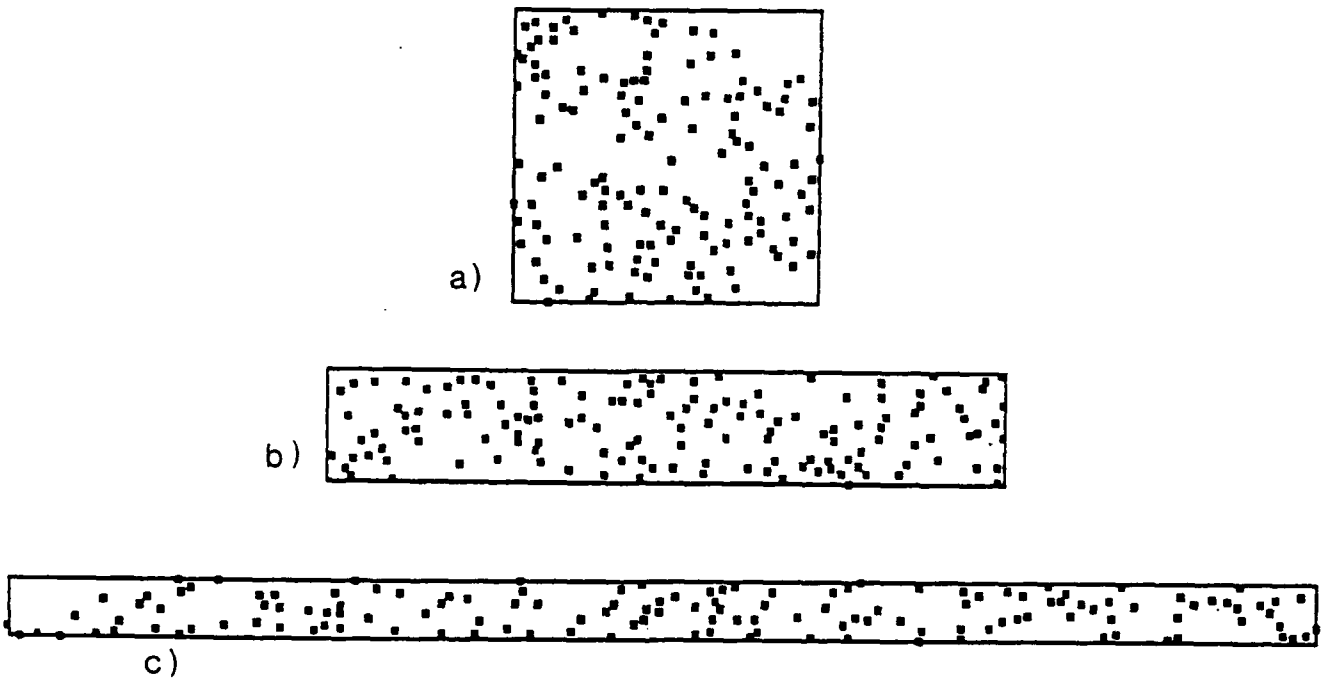

Figure 10. Scaled examples of random hole arrays containing 0.05 area fraction of 1.2 mm diameter holes with minimum allowable hole spacings of 0.5 mm and length-to-width ratios of (a) 1:1, (b) 5:1 and (c) 20:1. The tensile axis is horizontal.

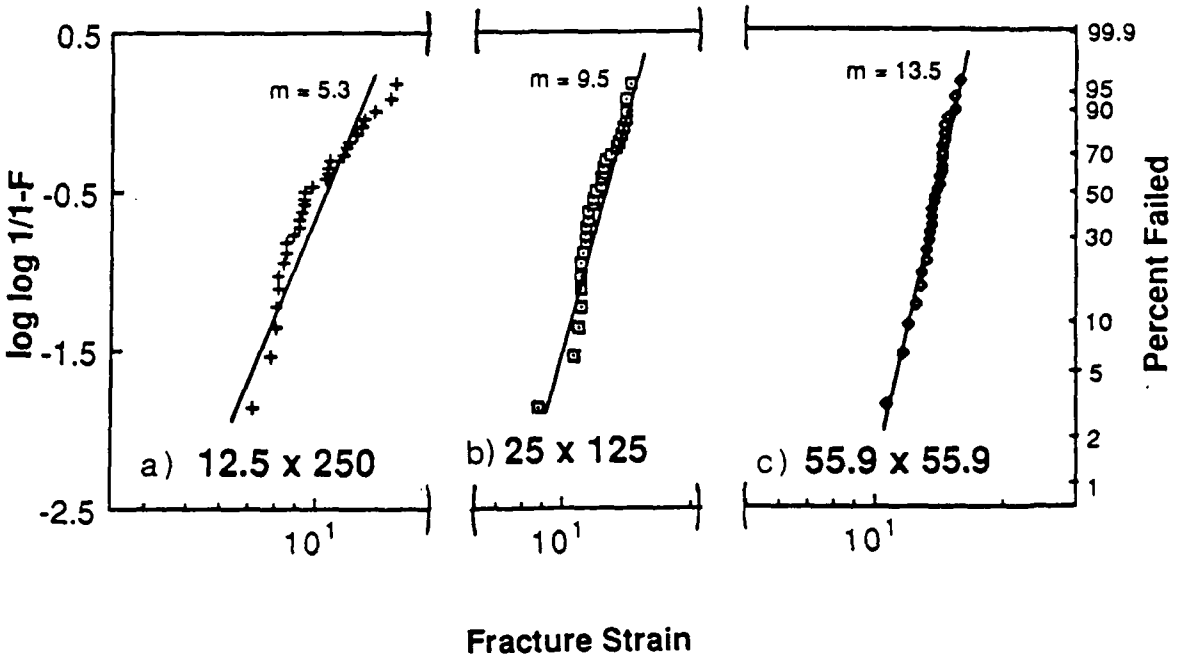

Figure 11. Weibull plots for 1100 aluminum specimens containing 0.01 area fraction of 2.0 mm diameter holes with a minimum allowable hole spacing of 0.5 mm and a specimen size of (a) 12.5x250, (b) 25x125 and (c) 55.9x55.9 mm.

the use of Weibull statistics. Clearly, the ductility data have a greater degree of scatter in long, narrow specimens (m=5.3) when compared to short, wide specimens (m=13.5). Finally, Figures 8a and 9a also show that the data is consistent with the normalized ductility of porous metals.[30,31]

The above results are fully consistent with imperfection theory as originally formulated for the localized necking of sheet metal by Marciniak and Kucyznski.[32] Imperfection analysis typically assumes a pre-existing imperfection which extends across the load-bearing cross-section of a strip or specimen undergoing plastic deformation. Normally in such an analysis, the severity of the imperfection is fixed at an initial value which, in our case, would be characteristic of the starting pore microstructure. We propose that in a ductile material containing porosity, there are (a) initial imperfections along the specimen length due to the pore distribution as well as (b) "linking-induced" imperfections which are created as the linking of pores removes load-bearing ligaments within the specimen. The total imperfection of the specimen is a result of a combination of the imperfections mentioned above.

The specimen shape and imperfection considerations discussed above contain implications to the effects of porosity on fracture toughness. Specifically, it is normally the case that porosity affects tensile ductility much more adversely than fracture toughness.[33,34] This effect may be understood in terms of the imperfection theory and specimen shape effects, particularly as regards the scale of the porosity and the size of the crack-tip plastic zone. During the onset of crack propagation, fracture occurs within a comparatively small volume of material defined by the plastic zone ahead of the crack tip. Given the scale of porosity, in effect failure occurs in a short "specimen" which is very wide, unless the crack is allowed to propagate in a very tortous path which by itself induces crack growth resistance. As a result, fracture toughness values of metals containing porosity are approximately equal to those of the fully dense material. In contrast, a large volume of material is under deformation in a tensile test and the specimen shape effects

discussed above are able to take place. Thus, the failure process in the tensile specimen is able to seek out paths coinciding with the most severe imperfections consisting of clustered, linked pores on planes of high pore content. The result is that even an isolated, small group of clustered pores is subjected to the plasticity conditions which will cause a linking-induced imperfection and in turn cause failure.

In addition to the above study, we have recently verified that the movement of the hole centers due to the macroscopic applied strains has no significant effect on the predicted elongation to failure. This is quite important as it validates the computer simulation data which has been obtained previously and provides a further measure of confidence in extending the simulations to predicting the effects of more realistic hole/void "microstructures".

3. Processing and Properties of Copper-Niobium Alloys (with Kevin Zeik, Ph.D. candidate and Dr. Iver Anderson, Ames Laboratory)

The operating systems of certain advanced structural systems, such as those encountered by the hypersonic space plane, impose a new set of extremely stringent requirements on the next generation of materials. In particular, the presence of sharp, cyclic thermal transients in structural components operating at high temperatures in the presence of hydrogen (such as those encountered by the engine components of the aforementioned aircraft) require not only high temperature strength, thermal stability, and resistance to environmental embrittlement but also a high degree of thermal conductivity. Conventional high conductivity alloys which derive their strength from either strain or precipitation hardening simply do not exhibit the required thermal stability. Therefore a new alloy must be considered, the basis of which is radically different from those currently available. This material must be able to meet the design requirements of the hypersonic space plane as well as other applications, such as high temperature connectors, requiring high conductivity and strength at elevated temperatures and sometimes in aggressive environments. A candidate material for such applications is the copper-niobium

microcomposite-type only. Not only are these materials estimated to meet the required demands, but they will be an effective model system which can be used to study the generic yielding and stress-strain response of this new type of alloy material.

The purpose of this study is to process into bulk form and subsequently investigate the properties and microstructure of a copper-based alloy formed from rapidly solidified, ultrafine powders. The high temperature microstructural stability as well as the associated deformation and fracture behavior will be studied in detail. The alloys under consideration are characterized by a high volume fraction (~20%) of discontinuous, nearly spherical niobium particles embedded in a continuous copper-rich matrix, within which the high temperature microstructural stability is derived from the mutual insolubility of the copper and niobium phases. The result is a very fine-scale particulate composite microstructure which should exhibit considerable particle or grain size strengthening, while retaining microstructural (and strength) stability to temperatures approaching 650°C. High pressure gas atomization will be used to attain the ultrafine (<10μm), rapidly solidified powders needed to produce the desired fine-scale microstructure. It is important to recognize that the powders produced are, in fact, composites themselves, in that the microstructure consists of discontinuous niobium-rich particles (<0.1μm) surrounded by a copper-rich matrix, which is subsequently contained within a thin, niobium-rich shell. Figure 12 shows an example of this preferred microstructure, which is a result of a monotectic solidification reaction induced by the effects of gas atomization (rapid solidification as well as undercooling of the molten alloy).

An essential goal of this project is to process these powders into bulk form, without destroying the fine scale of the powder's initial microstructure. Using hot isostatic pressing (HIPing), it appears feasible to attain a "microcomposite" alloy within which the niobium-rich particles would retain their small size and close spacing, such that, at the volume fractions employed (10 % - 25%), a large strengthening increment is obtained and retained to temperatures approaching 650°C.

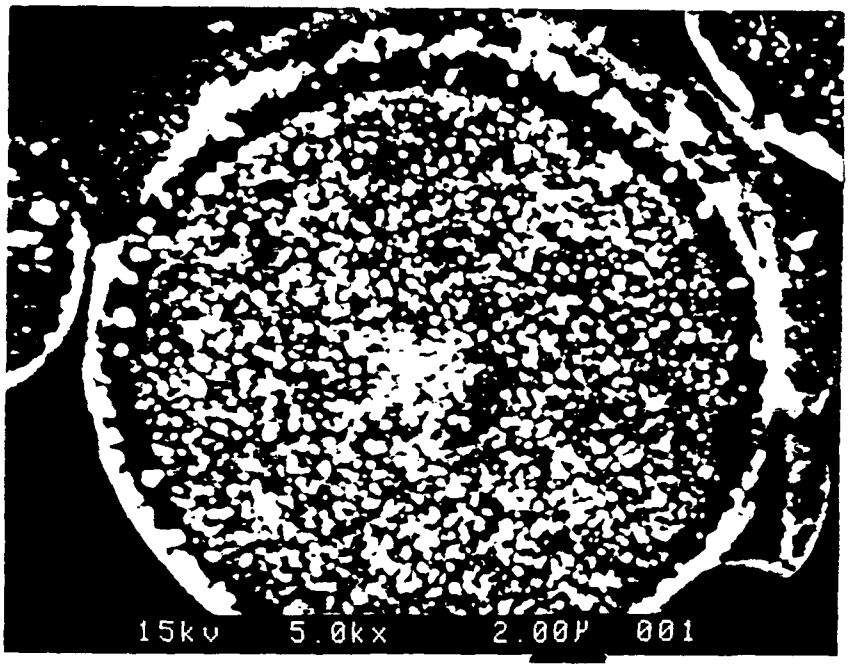

Figure 12. Scanning electron micrograph of a copper - 10 w/o niobium rapidly solidified powder particle (Powder Particle size = 20 µm).

A key element in the potential success of this program is the ability to process ultrafine powders solidified at sufficiently high rates and undercoolings to form the preferred, fine-scaled microstructures. This is being accomplished in a cooperative effort with Dr. Iver Anderson who recently joined the Ames Laboratory (USDOE), Iowa State University. Construction of a new atomizer, which will be used to produce the materials required for this study, has been completed within the last month. This atomizer, the design of which is greatly improved from the earlier version located at the Naval Research Laboratory, permits production of large quantities (>1kg) of ultrafine powder (<10μm). The atomizer benefits in many ways from a more efficient design which prevents turbulence and which employs a more efficient collector to improve ultrafine (<10μm) powder collection. The new atomizer is also constructed with a much larger power supply; this latter factor eliminates the previous problems encountered at NRL of Cu-Nb melt freezing in the pour tube before it can be atomized. To also aid in the delivery of molten metal through the pour tube, a secondary inductor has been fabricated and placed between the crucible wall and the induction coils of the furnace; this intensifies the energy delivered to the crucible and pour tube assembly.

Preliminary atomization experiments using the Ames Laboratory atomizer have very recently been done using pure copper in a stream of argon gas. The product powder was nearly spherical with a mean size of 14μm. Two attempts have also been made to atomize a copper-19.6 wt% niobium alloy, designed to yield 20 vol% of discrete niobium particles. The first attempt was interrupted when the cooling water supplied to the secondary inductor began to superheat. This problem was corrected by strategically placing zirconia felt insulation between the crucible and the secondary inductor. The second attempt was interrupted moments before the atomization was to begin when the thermocouple used to monitor melt temperature failed. This thermocouple failure was later traced to the disintegration of the alumina protection tube due to the intense (>1800°C) heat. This problem has since been corrected by using BeO refractory in place of the alumina, which

should extend the upper use temperature to well above 2300°C. The next attempt to produce powder from a Cu - 20 vol% Nb alloy is scheduled for early May. The charge weight will be approximately 1800 grams, which should produce a substantial amount of powder which has the desired, fine-scale microstructure.

Once the alloy powder has been obtained, microstructural characterization will be done to determine the range of powder size considered useable. It has been postulated from the work of Verheoven et al.[35] that the copper-niobium microstructures will be very sensitive to cooling rate and amount of undercooling, both of which are dependent on particle size. In the case of large powder sizes where cooling rates should be low, the microstructure will no longer consist of discrete, finely spaced niobium-rich particles surrounded by a copper matrix but rather should be characterized by a network of niobium dendrites in a copper matrix. As a result, we anticipate a substantial decrease in the maximum attainable strength of an alloy based on such large particle sizes. Preliminary evidence based on a Cu - 10 wt% Nb powder, which has been produced by Rocketdyne using centrifical atomization, indicates that the rapidly solidified powder does indeed have the preferred microstructure (Nb particle size ~0.1μm) in those powders particles up to about 30μm; see Figure 12. These observations suggest that the fine powders which we will produce by gas atomization at the Ames Laboratory will have a high useful yield. It may be recalled that in our earlier atomization experiment, the copper powder had a mean size of 14μm.

Subsequent to the atomization of the powders, the alloy powder will be cleaned to remove any surface oxide, placed into pure copper tubes and sealed. These will then be hot isostatically pressed (HIPed) to produce a fully dense microcomposite. This material will then be subject to microstructural stability investigations at temperatures up to 750°C utilizing both transmission and scanning electron microscopy to characterize the stability of the microstructure. In addition, both the deformation (monotonic stress-strain response) and fracture behavior will be studied over the temperature range of 27°C to 650°C. Other

pertinent behavior, notably electrical resistivity, will also be determined to help establish the validity of this material for its intended applications.

Although a goal of this project is to utilize novel processing to produce high strength, high conductivity materials for elevated temperature use, the mechanism of strengthening in these microcomposite-type alloys is of fundamental signifiance. While a particle strengthening component is expected, the large volume fraction of very closely spaced niobium particles suggest that additional strengthening mechanisms may be present and may even dominate the overall deformation response of the microcomposite. It is quite possible that a substantial grain-size type of strengthening may be present[36]. In addition, the close proximity and high volume fraction of niobium suggests a very high rate of strain hardening, resulting from the geometrically necessary dislocations[37]. To aid in this modeling, other compositions of the copper-niobium alloy will be attempted, such as the Cu-10vol% or Cu-30vol% alloys. Through an understanding of the strengthening and microstructural stability of the Cu-Nb system, it should be possible to establish constituitive relations predicting the flow and fracture behavior not only for this system, but also for other microcomposite alloys and composites which contain a high volume fraction of deformable particles with interparticle spacings in the 10-100nm scale.

REFERENCES

1. M. Cohen, B. H. Kear, and R. Mehrabian in Proc. of 2nd Int. Conf. on Rapid Solidification, Claitors Press, Baton Rouge, LA p. 1, 1980.
2. N. J. Grant, J. of Metals, 35, p. 20 (1983).
3. S. H. Whang, J. Mat'l. Sci., 21, p. 2224 (1986).
4. M. Eudier, Powder Metal., 9, pp. 278-290 (1962).
5. R. Haynes, Powder Metal., 1, pp. 17-20 (1977).
6. R. J. Bourcier, D. A. Koss, R. E. Smelser and O. Richmond, Acta Metall., 34 (12), pp. 2443-2453 (1986).
7. P. R. Smith, D. Eylon, S. W. Schewnker and F. H. Froes, Advanced Processing Methods for Titanium, Eds. D. F. Hasson and C. H. Hamilton (TMS-Warrendale), p. 61 (1981).
8. R. Haynes. The Mechanical Behavior of Sintered Alloys, (Freund Publishing House, London) 1981.
9. H. Neuber, Trans. ASME, p. 544 (1961).
10. S. S. Manson and M. H. Hirschberg, Fatigue: An Interdisciplinary Approach (Syracuse Univ. Press, Syracuse, NY) p. 133 (1964).
11. L. F. Coffin, Jr., Trans. ASM 561, p. 438 (1959).
12. D. A. Gerard and D. A. Koss, ONR Tech. Report No. 10, ONR CXontract No. N00014-86-K-0381, July 1988.
13. E. M. Dubensky and D. A. Koss, Metall. Trans A, 18A, p. 1887 (1987).
14. P. E. Magnusen, E. M. Dubensky and D. A. Koss, Acta Metal 36, p. 1503 (1988).
15. P. E. Magnusen, D. J. Srolovitz and D. A. Koss, Int. J. Fracture (to be published).
16. F. A. McClintock, J. of Appl. Mech., 35, p. 363 (1968).
17. A. Needleman, J. of Appl. Mech., 39, p. 964 (1962).
18. M. Nagumo, Acta Metall., 21, p. 1661 (1973).
19. B. I. Elelson, Trans. ASM, 56, p. 82 (1963).
20. P. F. Thomason, Acta Metall., 29, p. 763 (1981).
21. V. Tvergaard, Int. J. Frac., 17, p. 389 (1987) and 18, p. 237 (1982).
22. P. F. Thomason, Acta Metall., 33, pp. 1079 and 1087 (1985).

23. L. M. Brown and J. D. Embury, in Proc. 3rd Int. Conf. Strength of Metals and Alloys, p. 164 (1973).

24. R. A. Tait and D. M. R. Taplin, Scripta Met., 13, p. 77 (1979).

25. G. LeRoy, J. D. Embury, G. Edward and M. F. Ashby, Acta Metall., 29, p. 1509 (1981).

26. P. E. Magnusen, Ph.D. Thesis, Michigan Technological University, 1987.

27. K. S. Chan, D. A. Koss, and A. K. Ghosh, Met. Trans. A 15A, p. 323 (1983).

28. G. LeRoy and J. D. Embury in Formability (TMS-AIME, Warrendale, PA) p. 183 (1978).

29. A. Geltmacher and D. A. Koss, ONR Technical Report No. 11, ONR Contract No. N00014-86-K-0381, 1989.

30. K. M. Vedula and W. M. Heckel, Modern Developments in PowderMetallurgy, Vol. 12 eds. H. H. Hausner, H.W. Antes and G.D. Smith, MPIF, 1981.

31. B. I. Edelson and W. M. Baldwin, Trans. Am. Soc. Metals 55, p. 230 (1962).

32. Z. Marciniak and K. Kuczynski, Int. J. Mech. Sci 9, p. 609 (1967).

33. J. T. Barnby, D. C. Ghosh and K. Dinsdale, Powder Met., 16, 55, (1973).

34. N. R. Moody, W. M. Garrison and J. E. Swiggeresky, unpublished research.

35. J. D. Verhoeven and E. D. Gibson, J. Mat. Sci., 13, 1576 (1978).

36. W. A. Spitzig, to be published.

37. P. D. Funkenbusch, J. K. Lee and T. H. Courtney, Metall. Trans. A 18A, p. 1249 (1987).